O-Glycosylated Cell Wall Proteins Are Essential in Root Hair Growth

Silvia M. Velasquez,[1] Martiniano M. Ricardi,[1] Javier Gloazzo Dorosz,[1] Paula V. Fernandez,[2] Alejandro D. Nadra,[3] Laercio Pol-Fachin,[4] Jack Egelund,[5] Sascha Gille,[6] Jesper Harholt,[7] Marina Ciancia,[2] Hugo Verli,[4] Markus Pauly,[6] Antony Bacic,[8] Carl Erik Olsen,[9] Peter Ulvskov,[5] Bent Larsen Petersen,[5] Chris Somerville,[6] Norberto D. Iusem,[1,10] Jose M. Estevez[1]*

Root hairs are single cells that develop by tip growth and are specialized in the absorption of nutrients. Their cell walls are composed of polysaccharides and hydroxyproline-rich glycoproteins (HRGPs) that include extensins (EXTs) and arabinogalactan-proteins (AGPs). Proline hydroxylation, an early posttranslational modification of HRGPs that is catalyzed by prolyl 4-hydroxylases (P4Hs), defines the subsequent O-glycosylation sites in EXTs (which are mainly arabinosylated) and AGPs (which are mainly arabinogalactosylated). We explored the biological function of P4Hs, arabinosyltransferases, and EXTs in root hair cell growth. Biochemical inhibition or genetic disruption resulted in the blockage of polarized growth in root hairs and reduced arabinosylation of EXTs. Our results demonstrate that correct O-glycosylation on EXTs is essential for cell-wall self-assembly and, hence, root hair elongation in *Arabidopsis thaliana*.

Plant cell walls are complex and dynamic structures composed mostly of high-molecular-weight polysaccharides and highly glycosylated proteins (*1*, *2*). During plant growth, cells may expand up to 200 times their original length. During this process, the cell wall maintains its thickness through the addition of newly synthesized polysaccharides and proteins. Therefore, walls must possess sufficient tensile strength to withstand enormous turgor pressures (the driving force for growth) and involves controlled chemical modifications of wall constituents and wall networks. Approximately 1 to 2% of the *Arabidopsis* genome represents genes encoding putative enzymes that catalyze such modifications (*2*). Although the catalytic activity of the encoded protein is inferred from the predicted peptide sequence, the precise enzymatic function and biological role of many of these putative cell wall–modifying genes are unknown (*1*, *2*).

Cell walls contain abundant hydroxyproline-rich glycoproteins (HRGPs), a superfamily that encompasses extensins (EXTs) (*3*, *4*), proline-rich proteins (PRPs) (*4*), and arabinogalactan-proteins (AGPs) (*4*, *5*). These proteins undergo extensive posttranslational modification, which includes the modification of proline (Pro) residues to hydroxyproline (Hyp) by membrane-bound prolyl 4-hydroxylases (P4H2) (*6*). Nascent HRGPs are O-glycosylated (with arabinose and/or galactose) by glycosyltransferases (GTs) in the Golgi and endoplasmic reticulum (ER) (*7*–*11*) and are cross-linked into the wall by peroxidases through alternate Tyr residues to form a covalent network (*12*, *13*).

Root hair growth and proline hydroxylation. To study the function of HRGPs, we focused on root hairs because they represent a single cell type that plays an important role in nutrient absorption, and the growth morphology is easily

[1]Instituto de Fisiología, Biología Molecular y Neurociencias–Consejo Nacional de Investigaciones Científicas y Técnicas (IFIByNE-CONICET), Facultad de Ciencias Exactas y Naturales, Universidad de Buenos Aires, Buenos Aires C1428EGA, Argentina. [2]Cátedra de Química de Biomoléculas, Departamento de Biología Aplicada y Alimentos (Centro de Investigaciones en Hidratos de Carbono–CONICET), Facultad de Agronomía, Universidad de Buenos Aires, Buenos Aires CD1417DSE, Argentina. [3]Departamento de Química Biológica, Facultad de Ciencias Exactas y Naturales, Universidad de Buenos Aires, Buenos Aires C1428EGA, Argentina. [4]Programa de Pos-Graduação em Biologia Celular e Molecular, Centro de Biotecnologia, 91500–979, and Faculdade de Farmácia, Universidade Federal do Rio Grande do Sul, 90610–000, Brazil. [5]Department of Plant Biology and Biotechnology, Faculty of Life Sciences, University of Copenhagen, Copenhagen 1871, Denmark. [6]Energy Biosciences Institute, University of California, Berkeley, Berkeley, CA 94720, USA. [7]Department of Plant Biology and Biotechnology, Faculty of Life Sciences, University of Copenhagen, Copenhagen 1871, Denmark. [8]Plant Cell Biology Research Centre, School of Botany, University of Melbourne, Melbourne VIC 3010, Australia. [9]Department of Natural Sciences, Bioorganic Chemistry, Faculty of Life Sciences, University of Copenhagen, 1871, Denmark. [10]Departamento de Fisiología, Biología Molecular y Celular, Laboratorio de Fisiología y Biología Molecular (LFBM), Facultad de Ciencias Exactas y Naturales, Universidad de Buenos Aires, Buenos Aires C1428EGA, Argentina.

*To whom correspondence should be addressed. E-mail: jestevez@fbmc.fcen.uba.ar

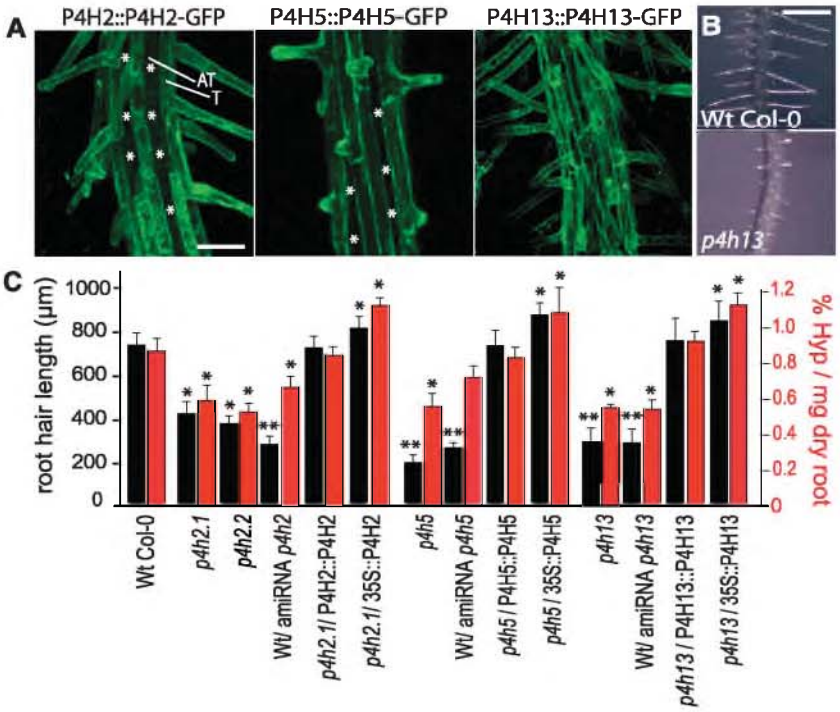

Fig. 1. *Arabidopsis* root hair growth is modulated by P4Hs. (**A**) Localization of GFP-tagged P4H2, P4H5, and P4H13 enzymes. GFP-tagged P4H2 and P4H5 are expressed in trichoblast cells (T), and GFP-tagged P4H13 is expressed in both trichoblast and atrichoblast (AT) root cells. Absence of GFP signal is indicated by asterisks. Scale bar, 200 µm. (**B**) Shorter root hairs in *p4h13* mutant. Scale bar, 800 µm. (**C**) Root hair length (black bars) and Hyp content (red bars) in roots of WT Col-0 (WT), *p4h* insertional mutants, silenced [artificial microRNA (amiRNA)], and rescued mutants. Complementation of each *p4h* mutant was achieved by the corresponding WT P4H driven by either its own endogenous promoter or the 35S promoter. *P* values of one-way analysis of variance (ANOVA) test, $*P < 0.01$, $**P < 0.001$.

observed with light microscopy. A link between P4Hs, glycosylation, and root hair phenotype was first suggested by results from an in vivo biochemical experiment that analyzed roots from plants carrying a green fluorescent protein (GFP)–tagged HRGP transgene (LeAGP1-GFP) (*14*) that were treated with either ethyl-3,4-dihydroxybenzoate (EDHB), which binds to the active site of AtP4Hs (fig. S1) (*15*), or α,α-dipyridyl (DP), which chelates the cofactor Fe^{2+} (*16*, *17*). This treatment caused an up to 50% inhibition of root hair growth at 48 to 219 nM (fig. S2) and the accumulation of the non-glycosylated ~42 kD form of LeAGP1-GFP rather than the fully O-glycosylated 150-to-200-kD form (fig. S2) (*14*).

We then characterized different members of the AtP4H family with distinct expression patterns, particularly those expressed in a tissue-specific manner in roots such as AtP4H2 and AtP4H5, which are expressed mainly in the root hair morphogenic zone (fig. S3 and table S1) (*18*, *19*), as well as AtP4H13, which is also expressed in roots (Fig. 1A). Cell-type expression analysis showed that GFP-tagged P4H2 and P4H5 are present only in trichoblast cells, whereas P4H13 is expressed in both trichoblast and atrichoblast cells (Fig. 1A). Subcellular localization of all three P4Hs was confined to the apical zone of emerging root hairs but was distributed throughout the cell in elongated root hairs (Fig. 2). At the subcellular level, all three P4Hs colocalized with an ER marker. P4H2 and P4H5 partially colocalized with a Golgi marker (fig. S4). To clarify the role of these P4Hs in developing root hairs, we used plants with transferred DNA (T-DNA) insertions (knockout lines) in each of these three AtP4H genes (fig. S5). We observed that the P4H-deficient lines displayed shorter-than-normal root hair length (Fig. 1B, fig. S5, and table S2), which mimicked the pharmacological inhibition of P4Hs that was previously reported (fig. S2). In addition, the *p4h2* mutant showed reduced root hair density. All three mutants lacked normal AtP4H transcripts, with the exception of *p4h2.1* (fig. S5) and showed reduced Hyp content in root cell walls in roots (Fig. 1C). Similar results were obtained by silencing normal AtP4H gene expression with complementary microRNA (Fig. 1C and fig. S5). Therefore, we concluded that the normal elongation of root hair cells requires Pro hydroxylation, performed by AtP4H enzymes, and the subsequent O-glycosylation of HRGPs, which is a consequence of Pro hydroxylation (*20*).

In support of the conclusions derived from *p4h* mutants, GFP-tagged P4Hs driven by either their own promoter (Fig. 1C and fig. S5) or the strong 35SCaMV constitutive promoter (Fig. 1C and table S2) restored root hair length, morphological phenotypes, and cell wall Hyp content to wild-type (WT) levels. Overexpression of P4Hs in a WT genetic background (fig. S6) doubled root hair length (Fig. 1D and fig. S6) and increased root hair density (fig. S7).

Given the overlapping substrate specificity of P4Hs (*6*), we explored the potential genetic interactions among P4Hs by observing the root hair phenotype that was displayed by double mutants (fig. S7). The *p4h2-p4h5* double mutant phenotype was similar to that of the single mutant *p4h5*, suggesting a functional overlap between P4H2 and P4H5. In contrast, the double mutant *p4h2-p4h13* line had shorter root hairs and exhibited a lower Hyp content in the cell walls than that of the respective single *p4h* mutant (fig. S7), suggesting subtle differences in substrate specificity for each of these P4Hs. To address the target specificity of P4H5, we performed a yeast two-hybrid screen using P4H5 as bait and identified LRX3, a root-specific leucine-rich-repeat extensin (At4g13340) and proteins containing polyproline II repeats (*25*) as targets of P4H5 (table S3). We calculated the interaction of each P4H (P4H2, P4H5, and P4H13) with the $(SP)_5$ and PAPAPSPT peptides that are present in AGPs or a polyproline repeat that is usually present in EXTs and PRPs [fig. S8, table S4, and supporting online material (SOM) text S1]. The modeling showed that these P4Hs have a high affinity of P4Hs for polyproline-like (EXT-PRP–type) substrates (fig. S8). Other biochemical studies have also demonstrated a greater hydroxylation activity on consecutive Pro residues compared with that on nonadjacent residues (*6*).

O-linked glycans in extensins. Having established the importance of P4Hs in posttranslational modifications of the EXT peptide backbone and considering that O-glycosylation is relevant in protein function either directly or indirectly through changes in polypeptide conformation, we explored O-glycosylation, mainly O-arabinosylation, in the context of EXT structure. Using genome-wide expression analysis, we determined that glycosyltransferases (GTs) RRA3 (reduced residual arabinose 3; At1g19360) and XEG113 (At2g35610) (fig. S9), both members of the GT family 77 (GT 77) of the Carbohydrate Active enZYme database (CAZY; www.cazy.org), were coexpressed with P4H2 and P4H5. RRA3 was 70 and 82% identical to the putative membrane-bound type-II arabinosyltransferases RRA1 and RRA2, respectively, which are implicated in EXT glycosylation (fig. S9) (*8*, *9*). The impaired root hairs that were exhibited by *rra1-rra3* mutants were similar to those of *p4h2*, *p4h5*, and *p4h13* mutants (Fig. 3A). In addition, *rra1-rra3* mutants had reduced EXT epitope content in their root cell walls (fig. S10). Another GT77 family member, XEG113 (At2g35610), which is a putative arabinosyltransferase, has also been reported to glycosylate EXTs (*10*). The *xeg113-2*

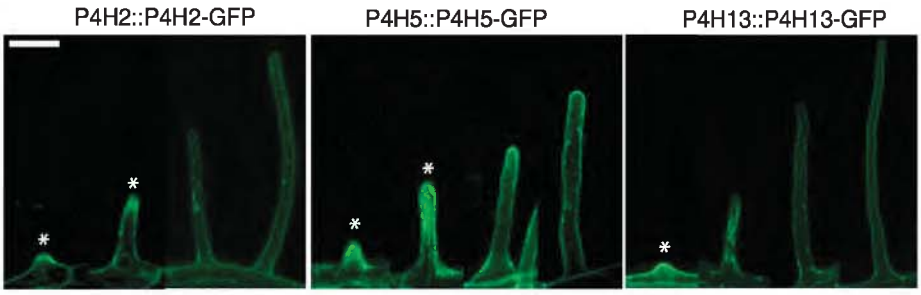

Fig. 2. Expression of GFP-tagged P4H2, P4H5, and P4H13 under the control of their respective endogenous promoters at different stages of root hair development. Scale bar, 200 μm.

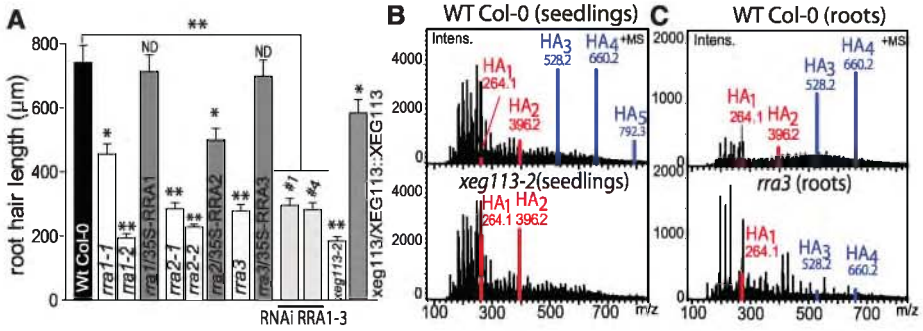

Fig. 3. EXT-associated arabinosyltransferases. (**A**) Root hair length (mean ± SEM) in *rra1-3/xeg113-2* mutants and their complemented lines. *P* values from one-way ANOVA test, $*P < 0.01$, $**P < 0.001$. (**B** and **C**) Mass-spectra of EXT O-glycans (Hyp-arabinosides, HA1-HA5) analyzed with ESI-MS on WT or mutant (B) seedlings and (C) roots. Hyp-arabinosides were detected as follows: HA5, Hyp-$(Ara)_5$; HA4, Hyp-$(Ara)_4$; HA3, Hyp-$(Ara)_3$; HA2, Hyp-$(Ara)_2$; and HA1, Hyp-$(Ara)_1$. Ions important for the interpretation of the results are highlighted in red (moieties containing up to two arabinose residues) or in blue (moieties containing three to five arabinose units, which are lacking or notably reduced in the mutants).

mutant also had reduced root hair growth (Fig. 3A) and lower levels of the EXT-type epitopes in root cell walls (fig. S10). As expected, *rra1-rra3* mutant phenotypes were partially to fully complemented by the WT gene that was driven by the 35*S* promoter, and the *xeg113-2* phenotype was also rescued by the WT gene that was driven by the XEG113 promoter (Fig. 3A). Reporter constructs revealed that these enzymes are present in Golgi and that this localization was abolished by brefeldin A (*21*), a Golgi-disrupting drug [for RRAs (fig. S9)]. Therefore, we conclude that P4H2, P4H5, and P4H13 hydroxylate EXTs, which are subsequently arabinosylated by the RRA1-RRA3/XEG113 enzymes to form native, fully glycosylated EXTs.

EXTs isolated from the *xeg113* mutant, not previously reported to be associated with root hair formation before this work, have shortened arabinosyl side chains (*10*). This glycosidic linkage analysis provided information on average composition rather than a specific sequence and/or distribution of the EXT oligoarabinosides that can vary from Hyp-$Ara_{(1-5)}$. Therefore, we used base-mediated peptide backbone hydrolysis and electrospray ionization-mass spectrometry (ESI-MS) to analyze in detail EXT glycopeptides (Hyp-O-glycans) from the GT mutant plants. *xeg113* has Hyp-$(Ara)_{1-2}$ side chains and lacks any of the WT Hyp-$(Ara)_{3-5}$ side chains (Fig. 3B and fig. S11), whereas *rra3* has a limited Hyp-$(Ara)_1$ side chain (Fig. 3C). We hypothesize that XEG113 and RRA3 incorporate the third and second arabinose, respectively, on the oligoarabinoside chain of EXTs (fig. S12) (*14*). On the basis of previous findings (*23*), we reasoned that absent or defective O-arabinosides on EXTs destabilize their helical secondary structure. Consequently, we analyzed conformational changes induced by Pro hydroxylation and O-arabinosylation of the EXT repetitive motif $Ser(Pro)_4$ using molecular dynamics simulation (fig. S13 and SOM text S2). The simulation showed that O-glycosylation stabilized the helical conformation of the $Ser(Hyp)_4$ peptide. In contrast, the defective O-glycosylated peptide in *xeg113* mutant (fig. S12) displayed two abnormal conformational states in solution (fig. S13) that may be expected to hamper EXT interactions with their surrounding environment, including interactions with other EXTs (*12*) or with target enzymes, such as peroxidases (*13*, *24*).

Root hair–specific extensins. Lastly, to further analyze the involvement of EXTs as P4H targets in root hair growth we screened the *Arabidopsis* genome for other genes that were co-expressed with root-specific or root-enriched EXTs. We identified the cell wall–related genes *AtEXP7,18*, *AtPRP1*, and *AtRHS13,18* (*25*–*27*), including the leucine-rich repeat extensin 1, *AtLRX1* (*24*), and several peroxidase genes [*AtPER13a,73* (fig. S14)]. Most of the EXTs identified here (table S5) have not been previously associated with root hair development. These extensins contain the Tyr-X-Tyr motif that forms intermolecular cross-links via peroxidases (*12*, *13*), enabling the structuring of a distinctive network in root hair cell walls (*12*, *28*, *29*). The transcription factor RSL4 (At1g27740), which is a regulator of root hair growth (*30*), appeared to control the expression of several of these EXTs (fig. S14 and table S5). EXT function in vivo was directly assessed by screening all the *ext* knockout mutants (fig. S15). Consistenly, several of the *ext* knockout mutants displayed a visible short-hair phenotype (fig. S16).

Conclusions. In the current study, our results suggest that EXT proteins in root hairs are first modified by P4H2, P4H5, and P4H13, which hydroxylate the Pro residues to Hyp, and subsequently by arabinosyltransferases XEG113/RRA1-3, which elongate the O-arabinosides. Once EXTs are secreted into the cell wall, mature EXTs form a network by the oxidative cross-linking of several Tyr residues (fig. S17) (*12*, *28*, *29*). This cross-linking is a critical step in cell wall self-assembly for root hairs and, perhaps, other wall types, such as pollen tubes. The role of EXTs in cell wall assembly is poorly understood. However, the functions of EXTs are not confined to root hairs or other tip-growing cells. Both AGPs and extensins play key roles in cell wall assembly through their interactions with pectic polysaccharides. Associations between AGPs and pectins have been observed in many cell types (*31*). A study of extensin AtEXT3 has suggested that extensins and pectin created a coacervate that served as template for further cell wall deposition (*12*), which is an idea that has been corroborated by in vitro studies (*32*). Our results on the exposed cell walls of developing root hairs indicate that the posttranslational modifications of O-glycosylated cell wall proteins are of broad importance to cell differentiation and plant development. Moreover, overexpression of the P4H genes increased root hair length and density, which may pose an option to increase plant biomass because of the essential function of root hairs in both nutrient and water assimilation.

References and Notes

1. D. J. Cosgrove, *Nat. Cell Biol. Rev* **6**, 850 (2005).
2. C. Somerville *et al.*, *Science* **306**, 2206 (2004).
3. J. F. Xu, L. Tan, D. T. Lamport, A. M. Showalter, M. J. Kieliszewski, *Phytochemistry* **69**, 1631 (2008).
4. M. J. Kieliszewski, D. T. A. Lamport, *Plant J.* **5**, 157 (1994).
5. A. M. Showalter, B. Keppler, J. Lichtenberg, D. Gu, L. R. Welch, *Plant Physiol.* **153**, 485 (2010).
6. P. Tiainen, J. Myllyharju, P. Koivunen, *J. Biol. Chem.* **280**, 1142 (2005).
7. K. Yuasa, K. Toyooka, H. Fukuda, K. Matsuoka, *Plant J.* **41**, 81 (2005).
8. B. L. Petersen *et al.*, *Annu. Plant. Rev* **41**, 305 (2011).
9. J. Egelund *et al.*, *Plant Mol. Biol.* **64**, 439 (2007).
10. S. Gille, U. Hänsel, M. Ziemann, M. Pauly, *Proc. Natl. Acad. Sci. U.S.A.* **106**, 14699 (2009).
11. E. Shpak, J. F. Leykam, M. J. Kieliszewski, *Proc. Natl. Acad. Sci. U.S.A.* **96**, 14736 (1999).
12. M. C. Cannon *et al.*, *Proc. Natl. Acad. Sci. U.S.A.* **105**, 2226 (2008).
13. M. A. Held *et al.*, *J. Biol. Chem.* **279**, 55474 (2004).
14. J. M. Estévez, M. J. Kieliszewski, N. Khitrov, C. Somerville, *Plant Physiol.* **142**, 458 (2006).
15. K. Majamaa, V. Günzler, H. M. Hanauske-Abel, R. Myllylä, K. I. Kivirikko, *J. Biol. Chem.* **261**, 7819 (1986).
16. N. Barnett, *Plant Physiol.* **45**, 188 (1970).
17. Materials and methods are available as supporting material on *Science* Online.
18. K. D. Birnbaum *et al.*, *Science* **302**, 1956 (2003).
19. S. M. Brady *et al.*, *Science* **318**, 801 (2007).
20. M. J. Kieliszewski, *Phytochemistry* **57**, 319 (2001).
21. C. Ritzenthaler *et al.*, *Plant Cell* **14**, 237 (2002).
22. J. P. Stafstrom, L. A. Staehelin, *Plant Physiol.* **81**, 242 (1986).
23. N. W. Owens, J. Stetefeld, E. Lattová, F. Schweizer, *J. Am. Chem. Soc.* **132**, 5036 (2010).
24. N. J. Price *et al.*, *J. Biol. Chem.* **278**, 41389 (2003).
25. N. Baumberger *et al.*, *Plant Physiol.* **131**, 1313 (2003).
26. N. Baumberger, M. Steiner, U. Ryser, B. Keller, C. Ringli, *Plant J.* **35**, 71 (2003).
27. S.-K. Won *et al.*, *Plant Physiol.* **150**, 1459 (2009).
28. D. T. A. Lamport, M. J. Kieliszewski, Y. Chen, M. C. Cannon, *Plant Physiol.* **156**, 11 (2011).
29. C. Ringli, *Plant J.* **63**, 662 (2010).
30. K. Yi, B. Menand, E. Bell, L. Dolan, *Nat. Genet.* **42**, 264 (2010).
31. P. Immerzeel, M. M. Eppink, S. C. de Vries, H. A. Schols, A. G. J. Voragen, *Physiol. Plant.* **128**, 18 (2006).
32. R. Valentin *et al.*, *Langmuir* **26**, 9891 (2010).

Acknowledgments: We thank R. A. Fernandez for his assistance in confocal microscopy, S. Maldonado and S. Petrucelli for providing the access to a stereoscope, and A. Nebenführ for providing vectors of the ER and Golgi markers. This work was supported by grants from Agencia Nacional de Promoción Científica y Tecnológica (ANPCyT) (PICT2007-732 and PICT2006-983) and CONICET (PIP2812, PIP0890, and PIP0071) to A.D.N., N.D.I., and J.M.E.; from the Danish Agency for Science Technology and Innovation from the Danish Agency for Science Technology and Innovation (274-09-0082, 2101-07-0071) to J.E, P.U., and B.L.P; from the Australian Research Council to A.B.; and Conselho Nacional de Desinvolvimento Científic e Tecnológico (CNPq) and Coordenação de Aperfeiçoamento de Pessoal de Nível Superior (CAPES) to L.F. and H.V. We thank Arabidopsis Biological Resource Center (Ohio University) for providing T-DNA lines seed lines. Thanks to K. Kobayashi and M. Otegui for critical reading of the manuscript. This work was partially supported by a grant from the U.S. Department of Energy (DOE-FG02-03ER20133) and funding from the Energy Biosciences Institute to C.S. S.M.V. performed most of the experiments. M.M.R. analyzed and performed some of the experiments and analyzed the data. J.G.D. performed some of the experiments. P.V.F and M.C. quantified Hyp in mutants and transgenic lines. S.G. and M.P. provided the XEG113-GFP data and xeg113-2 mutant. A.D.N. performed molecular modeling of P4Hs. L.F. and H.V. measured the molecular dynamics of EXT peptides. J.E. and A.B. assessed the Golgi localization of RRAs proteins. C.E.O., P.U., and B.L.P. characterized *rra3* and *xeg113* EXTs using ESI-MS, and P.U. and B.L.P. isolated *rra1-3* RNAi and *rra3* mutants. C.S. analyzed the data. N.D.I. analyzed the data and wrote the paper. J.M.E. designed research, performed most of the experiments, analyzed the data, supervised the project, and wrote the paper. The authors declare no competing financial interests.

Supporting Online Material

www.sciencemag.org/cgi/content/full/332/6036/1401/DC1
Materials and Methods
SOM Text S1 and S2
Figs. S1 to S17
Tables S1 to S6
References (*33*–*68*)

7 April 2011; accepted 10 May 2011
10.1126/science.1206657